Supporting Information

Accessing Perfluoroalkyl Nickel(II), (III), and (IV) Complexes Bearing a Readily Attached [C_4F_8] Ligand

Siqi Yu,[a] Yulia Dudkina,[b] Huan Wang,[a] Kirill V. Kholin,[b] Marsil K. Kadirov, [b] Yulia Budnikova,[b] David A. Vicic*[a]

[a] Department of Chemistry, Lehigh University, 6 E. Packer Ave., Bethlehem, PA 18015 (USA), E-mail: vicic@lehigh.edu

[b] A.E. Arbuzov Institute of Organic and Physical Chemistry, Kazan Scientific Center of Russian Academy of Sciences, 8, Arbuzov Str., 420088 Kazan (Russian Federation)

1. EPR anaylsis of [(tpy)Ni(C_4F_8)(CH_3CN)][BF_4] (7)

Solid-State:

Room temperature:

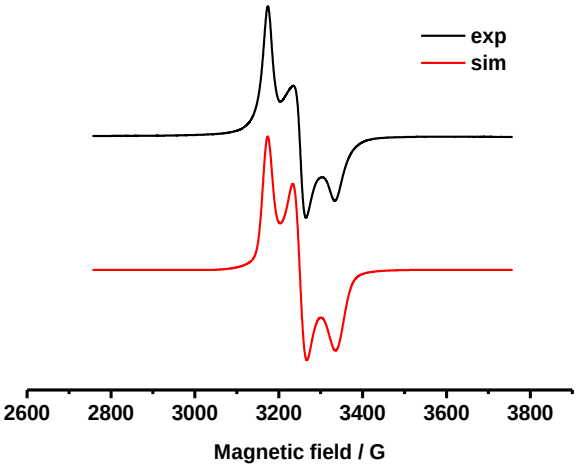

Figure S1: Solid state EPR spectrum of **7**.

$g_1 = 2.175$, $\Delta H_1 = 21$ G

$g_2 = 2.123$, $\Delta H_2 = 25$ G

$g_3 = 2.067$, $\Delta H_3 = 35$ G

The simulation reveals a rhombic symmetry of the complex. <g> = 2.122 is almost coincident with g-factors of the complex in THF and acetonitrile solutions. Therefore, the complex being dissolved, the first coordination sphere remains the same.

Temperature dependence:

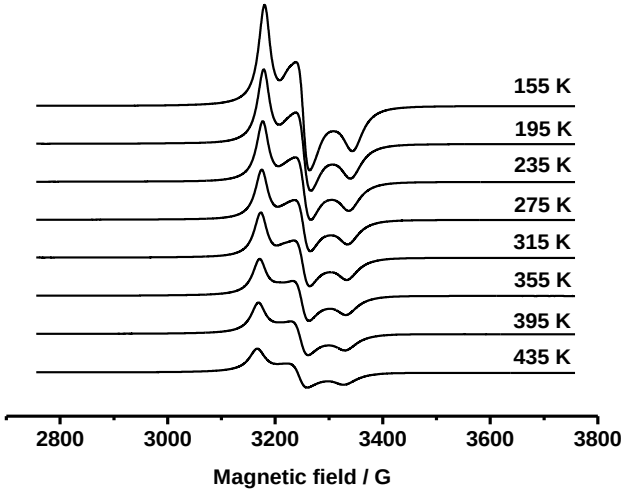

Figure S2: Temperature dependence of the solid state EPR spectrum of **7**.

The linewidth of the spectrum increases with the increase of temperature because of new degrees of freedom.

Acetonitrile solution:

Room temperature:

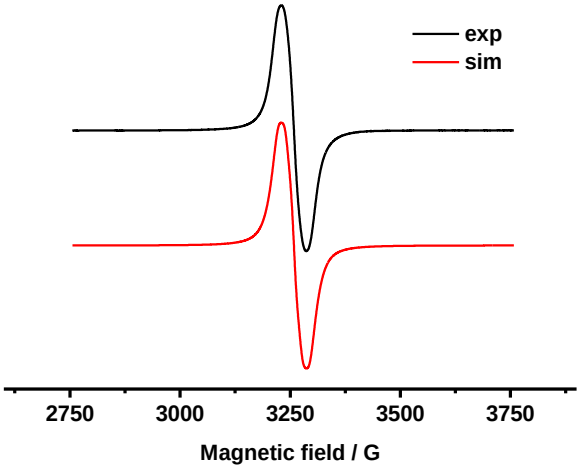

Figure S3: Room temperature EPR spectrum of **7** in MeCN.

$g_{NiCH3CN} = 2.121$

$a_N = 15$ G (two N atoms)

$\Delta H = 20$ G

The ESR spectrum is represented by a single homogeneously broadened line. The most accurate fitting is based on a simulation with hyperfine coupling constants obtained in acetonitrile solution at 235 K.

Temperature dependence:

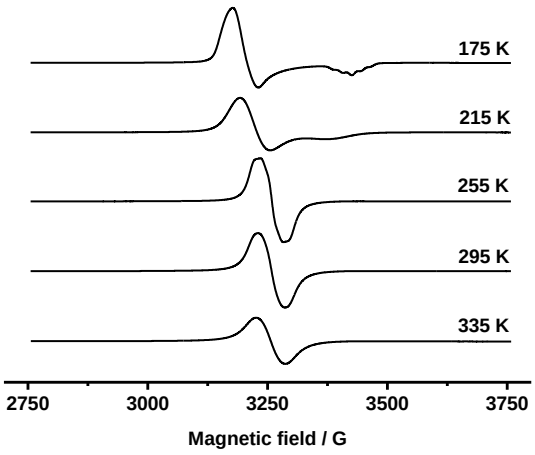

Figure S4: Temperature dependence of the EPR spectrum of **7** in MeCN solution.

The linewidth of the spectrum increases with the increase of temperature mostly by spin-rotation mechanism. At 235-255 K hyperfine splitting is observed. An anisotropic axial spectrum was recorded in a frozen solution.

235 K in MeCN:

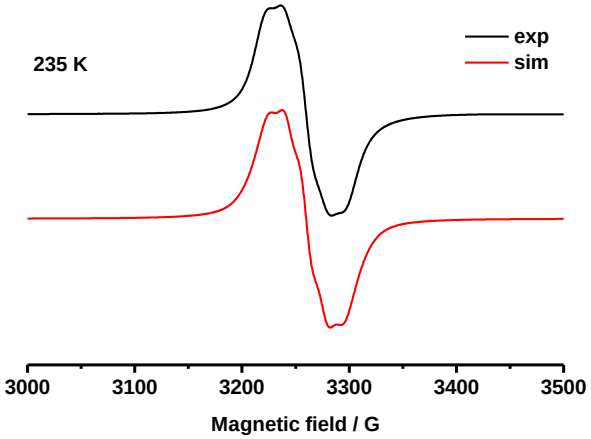

Figure S5: EPR spectrum of **7** in MeCN at 235 K.

At 235 K the linewidth of the spectrum is optimal to find:

$g = 2.119$

$a_N = 15$ G (two N atoms)

$\Delta H = 16$ G

Frozen solution (155 K) in MeCN:

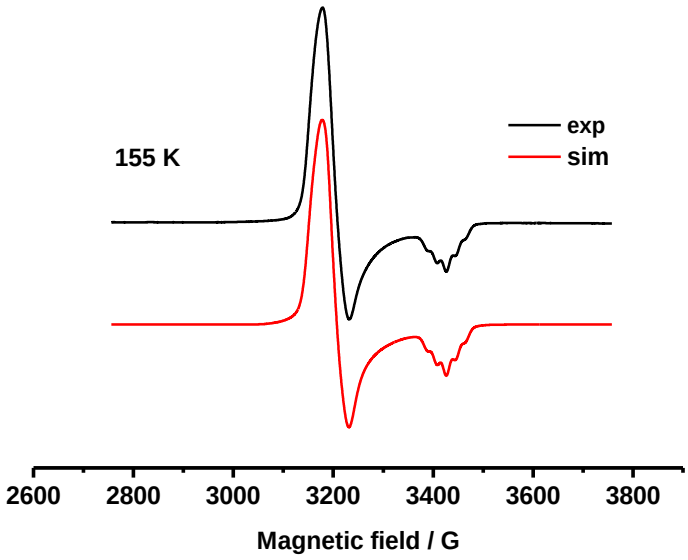

Figure S6: EPR spectrum of **7** in MeCN at 155 K.

An axial spectrum was recorded in a frozen solution (in contrast to the spectrum of the solid complex). <g> = 2.117 is almost coincident with the g-factor of the complex in solid state:

$g_{\parallel}$ = 2.017; a_N = 19 G (two N atoms); ΔH = 14 G

$g_{\perp}$ = 2.166; a_N = 15 G (two N atoms); ΔH = 21 G

THF solution:

Room temperature:

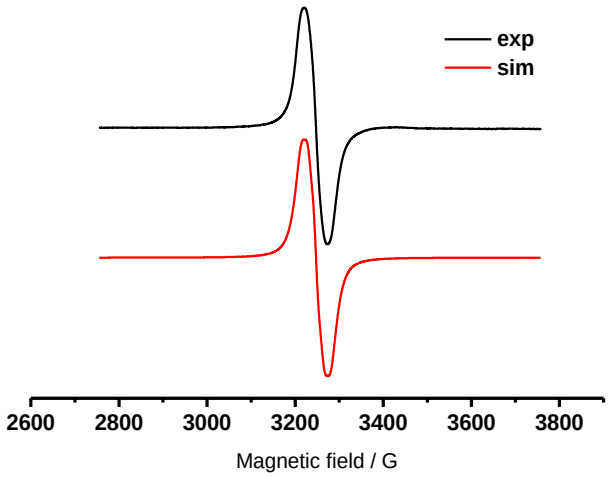

Figure S7: Room temperature EPR spectrum of **7** in THF.

The EPR spectrum is represented by a single homogeneously broadened line. The simulation was carried out likewise the one in acetonitrile solution.

$g_{NiCH3CN} = 2.128$

$a_N = 14.2$ G (two N atoms)

$\Delta H = 18$ G

Temperature dependence:

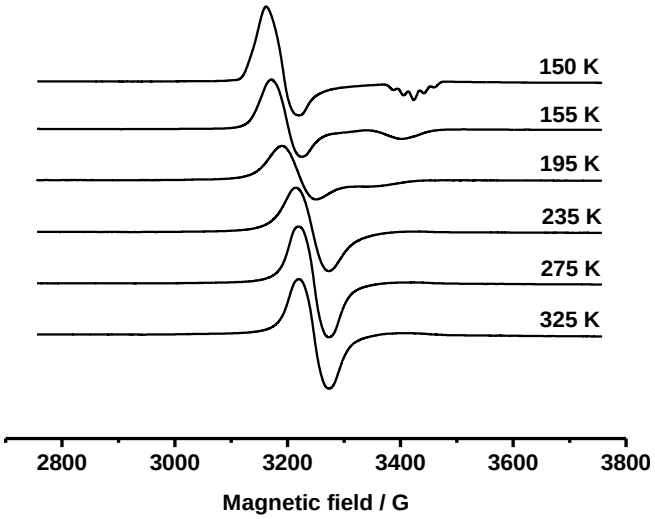

Figure S8: variable temperature EPR spectra of **7** in THF.

The linewidth of the spectrum increases with the increase of temperature mostly by spin-rotation mechanism. As the temperature decreases, g-tensor anisotropy dominates that results in spreading of the linewidth. An anisotropic spectrum (pertaining to an axially symmetric complex) was recorded in a frozen solution.

Frozen THF solution (150 K):

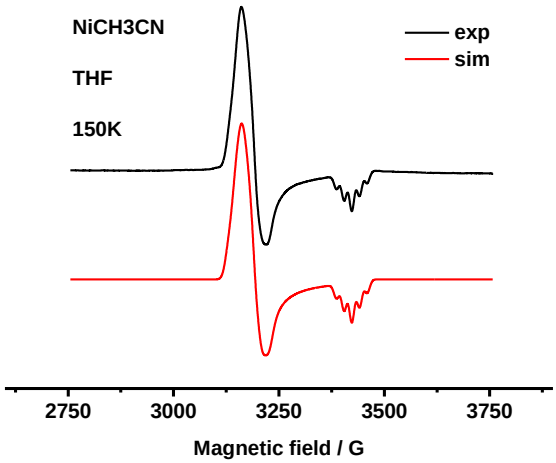

Figure S9: Room temperature EPR spectrum of **7** in THF.

An axial spectrum was recorded in a frozen solution (in contrast to the spectrum of the solid complex). <g> = 2.117 is almost coincident with the g-factor of the complex in solid state:

$g_1 = 2.1862$; $a_N = 15$ (two N atoms); $\Delta H = 17$ G

$g_2 = 2.1666$; $a_N = 15$ (two N atoms); $\Delta H = 17$ G

$g_3 = 2.0190$; $a_N = 18.2$ (two N atoms); $\Delta H = 12$ G

2. X-ray Crystallography

All crystals were placed on slides and then immersed in Paratone-N oil inside of a glovebox before examination under a microscope. The selected crystals were mounted on loops and then cooled to the appropriate temperature before data collection. Cif files for compounds **5 - 7** have been included in the Supporting Information. Crystallographic data (excluding structure factors) for compounds **5 - 7** have been deposited with the Cambridge Crystallographic Data Centre as supplementary publication numbers CCDC 1062817, 1062818, and 1062819, respectively. Copies of the data can be obtained free of charge on application to CCDC, 12 Union Road, Cambridge CB2 1EZ, UK [fax: +44 1223 336 033; e-mail: deposit@ccdc.cam.ac.uk].
:

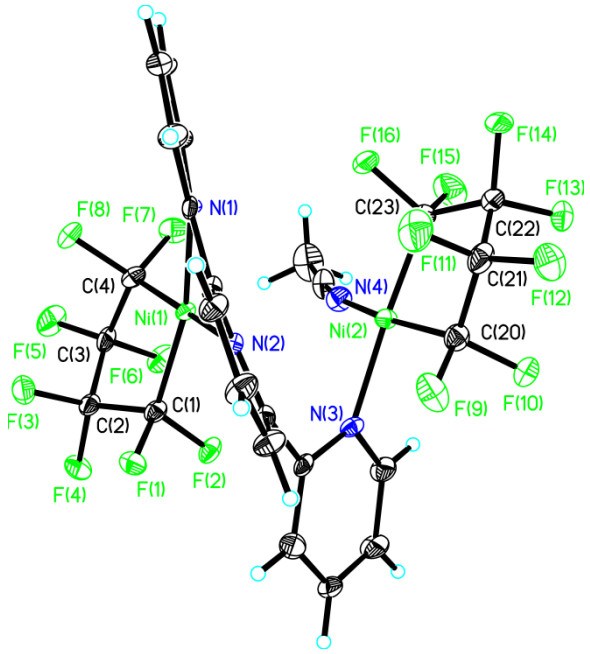

Figure S10. ORTEP diagram of [(tpy)$Ni_2(C_4F_8)_2$(MeCN)] (**5**). Co-crystallized THF solvent molecule omitted for clarity. Selected bond lengths (Å): Ni1-C4 1.909(10); Ni1-C1 1.918(10); Ni1-N1 1.956(8); Ni1-N2 1.985(9); Ni2-C20 1.895(11) Ni2-C23 1.908(11); Ni2-N4 1.918(10); Ni2-N3 1.953(9). Selected bond angles (°): C4-Ni1-C1 85.0(5); C4-Ni1-N1 93.6(4); C1-Ni1-N1 165.7(4); C4-Ni1-N2 173.3(4); C1-Ni1-N2 97.5(4); N1-Ni1-N2 82.4(4); C20-Ni2-C23 85.8(5); C20-Ni2-N4 167.9(5); C23-Ni2-N4 89.5(5); C20-Ni2-N3 91.4(4); C23-Ni2-N3 176.7(4); N4-Ni2-N3 92.9(4).

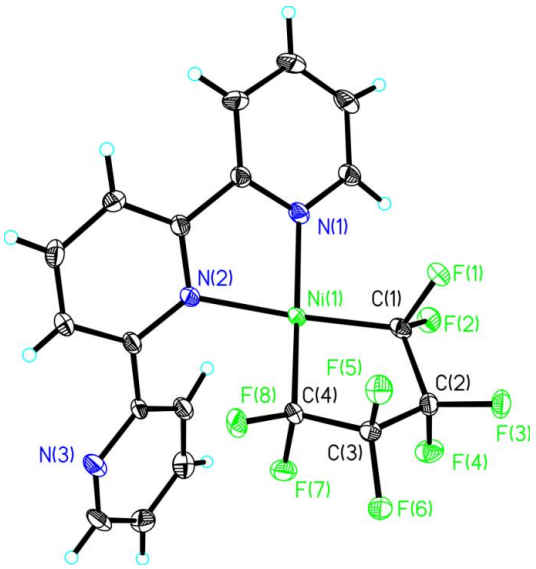

Figure S11. ORTEP diagram of [(tpy)Ni(C_4F_8)] (**6**). Selected bond lengths (Å): Ni1-C1 1.901(4); Ni1-C4 1.918(4); Ni1-N1 1.955(3); Ni1-N2 1.978(3). Selected bond angles (°): C1-Ni1-C4 85.42(16); C1-Ni1-N1 95.33(14); C4-Ni1-N1 166.44(15); C1-Ni1-N2 174.57(15); C4-Ni1-N2 96.40(14); N1-Ni1-N2 81.70(13).

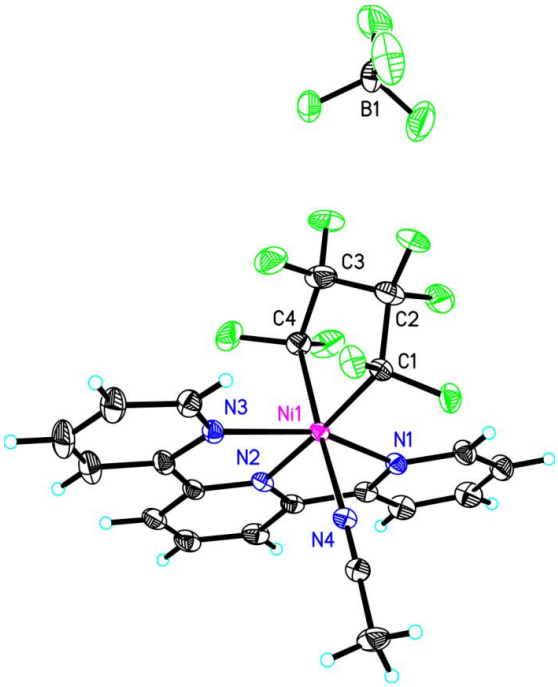

Figure S12. ORTEP diagram of [(tpy)Ni(C_4F_8)(MeCN)[BF_4] (**7**). Selected bond lengths (Å): Ni1-C1 1.966(3); Ni1-C4 1.960(4); Ni1-N1 2.163(3); Ni1-N2 1.964(3); Ni1-N3 2.172(3); Ni1-N4 1.966(3). Selected bond angles (°): C4-Ni1-N2 89.51(14); C4-Ni1-N4 173.75(14); N2-Ni1-N4 96.40(12); C4-Ni1-C1 84.61(15); N2-Ni1-C1 173.74(13); N4-Ni1-C1 89.55(14); C4-Ni1-N1 93.81(14); N2-Ni1-N1 78.11(12); N4-Ni1-N1 89.38(12); C1-Ni1-N1 100.09(13); C4-Ni1-N3 91.49(14); N2-Ni1-N3 78.25(12); N4-Ni1-N3 87.77(12); C1-Ni1-N3 103.99(13); N1-Ni1-N3 155.72(12).

3. Electronic structure calculations: Quantum calculations were performed with the Gaussian09W software.[1] Unconstrained geometry optimizations were performed using the spin unrestricted B3LYP exchange-correlation functional.[2,3] The m6-31G* basis set was used for nickel,[4] and the 6-31g* was used for all other atoms. All calculations have been checked for the absence of imaginary frequencies.

Table S1. Optimized Cartesian Coordinates for **7**.

Row	Symbol	X	Y	Z
1	Ni	11.01425	5.096689	10.50862
2	F	10.50447	6.390999	12.89207
3	F	10.4066	7.718084	11.15637
4	F	8.074145	6.880118	10.4331
5	F	7.949821	6.856292	12.63336
6	F	6.990607	4.52444	11.20124
7	F	8.589743	4.237805	12.6889
8	F	8.694219	4.400083	9.19363
9	F	9.359939	2.874539	10.60973
10	N	10.8406	5.989491	8.516117
11	N	11.81604	3.680949	9.340454
12	N	11.72327	3.616869	11.98162
13	N	12.74776	6.109111	10.77354
14	C	10.08458	6.459009	11.59063
15	C	8.553072	6.295949	11.56665
16	C	8.280466	4.790045	11.4827
17	C	9.24345	4.217553	10.4248
18	C	10.30225	7.167026	8.17802
19	H	9.991676	7.801882	8.996776
20	C	10.13152	7.562386	6.851025
21	H	9.686253	8.525987	6.628383
22	C	10.53373	6.695093	5.839757
23	H	10.41073	6.962497	4.79487
24	C	11.09528	5.467519	6.187662
25	H	11.40649	4.776811	5.412969
26	C	11.23623	5.141619	7.538786
27	C	11.81869	3.860081	8.006035
28	C	12.35135	2.880118	7.161847
29	H	12.35994	3.01355	6.087254
30	C	12.87765	1.721512	7.726792
31	H	13.29483	0.947359	7.09051
32	C	12.87139	1.559134	9.109584
33	H	13.28523	0.661863	9.552464
34	C	12.32397	2.570471	9.906059
35	C	12.25644	2.524282	11.38729
36	C	12.70439	1.431861	12.13432
37	H	13.124	0.559297	11.64804

38	C	12.59732	1.467977	13.52369
39	H	12.93653	0.626166	14.11931
40	C	12.04512	2.593692	14.12715
41	H	11.93615	2.664732	15.20393
42	C	11.61875	3.645271	13.3155
43	H	11.17032	4.5342	13.73753
44	C	13.67338	6.766978	10.98393
45	C	14.83233	7.608269	11.25427
46	H	15.32563	7.879656	10.31585
47	H	15.54385	7.073494	11.89088
48	H	14.51161	8.521214	11.76603

4. Synthetic Procedures:

General Considerations: All manipulations were performed using standard Schlenk and high vacuum techniques or in a nitrogen filled glovebox. Solvents were purified by passing through activated alumina and/or copper in a solvent purification system supplied by Pure Process Technology. 1,4-dibromooctafluorobutane was purchased from SynQuest Labs, Inc. and used without further purification. Solution ^{1}H NMR spectra were recorded at ambient temperature on a Bruker DRX 500 MHz spectrometer and referenced to residual proton solvent signals. ^{13}C NMR spectra were recorded on a Bruker NMR spectrometer operating at 125 MHz and referenced to solvent signals. ^{19}F spectra were recorded on the Bruker NMR spectrometer operating at 470 MHz. A Bruker D8 Quest diffractometer was used for X-ray crystal structure determinations. Elemental Analyses were performed at Midwest Microlab, LLC.

Preparation of [(tpy)Ni$_2$(C_4F_8)$_2$(MeCN)·THF] (5): Terpyridine (58 mg, 0.25 mmol) was dissolved in 4 mL of THF and was added dropwise to a stirred solution of **(**$(MeCN)_2Ni(C_4F_8)$ (170 mg, 0.50 mmol) in 8 mL of THF. The resulting mixture was stirred for 12 hours at room temperature, and then the volatiles were removed under vacuum. The residue was washed with pentane and dried, yielding a yellow solid. (Yield: 158 mg, 85%) Molecule displays paramagnetism: 1.00 μ_B in MeCN. Anal. Calcd (found) for THF solvate (co-crystalized in X-ray structure): $C_{29}H_{22}F_{16}N_4Ni_2O$: C, 40.32 (39.21) ; H, 2.57 (2.40).

Preparation of [(tpy)Ni(C_4F_8)] (6): Terpyridine (117 mg, 0.5 mmol) was dissolved in 4 mL of THF and added dropwise to a stirred solution of $(MeCN)_2Ni(C_4F_8)$ (170 mg, 0.50 mmol) in 8 mL of THF. The mixture was stirred for 12 hours at room temperature, and then the volatiles were removed under vacuum. The residue was washed with pentane and dried, yielding a yellow solid. (Yield: 218 mg, 89 %). Molecule displays paramagnetism: 1.16 μ_B in MeCN. Anal. Calcd (found) for $C_{19}H_{11}F_8N_3Ni$: C, 46.38 (46.11); H, 2.25 (2.33).

Preparation of [(tpy)Ni(C_4F_8)(MeCN)[BF_4] (7): A solution of $AgBF_4$ (119 mg) in THF was added dropwise to a (tpy)Ni(C_4F_8) (300 mg) solution in THF-CH_3CN at room temperature and the mixture was stirred for 3 h (turned blue), then filtered. The solution was concentrated and mixed with THF. Dry pentane was added slowly into the filtrate. The mixture was left in a freezer. The product was obtained as blue crystals (200 mg, 53%). Molecule displays paramagnetism: 1.77 μ_B in MeCN. Anal. Calcd (found) for $C_{21}H_{14}BF_{12}N_4Ni$: C, 40.69 (39.62) ; H, 2.28 (2.20).

References:

1) Frisch, M. J.; Trucks, G. W.; Schlegel, H. B.; Scuseria, G. E.; Robb, M. A.; Cheeseman, J. R.; Scalmani, G.; Barone, V.; Mennucci, B.; Petersson, G. A.; Nakatsuji, H.; Caricato, M.; Li, X.; Hratchian, H. P.; Izmaylov, A. F.; Bloino, J.; Zheng, G.; Sonnenberg, J. L.; Hada, M.; Ehara, M.; Toyota, K.; Fukuda, R.; Hasegawa, J.; Ishida, M.; Nakajima, T.; Honda, Y.; Kitao, O.; Nakai, H.; Vreven, T.; Montgomery, J., J. A.; Peralta, J. E.; Ogliaro, F.; Bearpark, M.; Heyd, J. J.; Brothers, E.; Kudin, K. N.; Staroverov, V. N.; Kobayashi, R.; Normand, J.; Raghavachari, K.; Rendell, A.; Burant, J. C.; Iyengar, S. S.; Tomasi, J.; Cossi, M.; Rega, N.; Millam, N. J.; Klene, M.; Knox, J. E.; Cross, J. B.; Bakken, V.; Adamo, C.; Jaramillo, J.; Gomperts, R.; Stratmann, R. E.; Yazyev, O.; Austin, A. J.; Cammi, R.; Pomelli, C.; Ochterski, J. W.; Martin, R. L.; Morokuma, K.; Zakrzewski, V. G.; Voth, G. A.; Salvador, P.; Dannenberg, J. J.; Dapprich, S.; Daniels, A. D.; Farkas, Ö.; Foresman, J. B.; Ortiz, J. V.; Cioslowski, J.; Fox, D. J. *Gaussian 09 for Windows, Revision C.01*; Gaussian, Inc., Wallingford, CT, 2009.

2) Becke, A. D. *J. Chem. Phys* **1993**, *98*, 5648.

3) Lee, C.; Yang, W.; Parr, R. G. *Phys. Rev. B: Condens. Matter* **1988**, *37*, 785.

4) Mitin, A. V.; Baker, J.; Pulay, P. *J. Chem. Phys.* **2003**, *118*, 7775.